We are IntechOpen,
the world's leading publisher of
Open Access books
Built by scientists, for scientists

6,900
Open access books available

185,000
International authors and editors

200M
Downloads

Our authors are among the

154
Countries delivered to

TOP 1%
most cited scientists

12.2%
Contributors from top 500 universities

CLARIVATE ANALYTICS
BOOK CITATION INDEX
INDEXED

WEB OF SCIENCE™

Selection of our books indexed in the Book Citation Index
in Web of Science™ Core Collection (BKCI)

Interested in publishing with us?
Contact book.department@intechopen.com

Numbers displayed above are based on latest data collected.
For more information visit www.intechopen.com

Laser- Assisted Machining of Difficult to Cut Materials

Damian Przestacki

Additional information is available at the end of the chapter

Abstract

The chapter presents the results of experimental investigation of the machinability of difficult to cut materials, e.g. silicon carbide particulate, aluminium metal matrix composite, cemented carbides layers, technical ceramics (Si_3N_4). The work focuses on the study of machinability during conventional and laser-assisted turning. Nowadays, the difficult to cut materials have a great application in different fields of industry, e.g. automobile or aerospace. Metal matrix composites are known as the difficult to machine materials, because of the hardness and abrasive nature element—in this case —SiC.

The work reported concentrates on the machinability improvement of difficult to cut materials by laser-assisted machining (LAM) when compared with conventional cutting process. Influence of laser beam during laser-assisted turning on temperature of the heating area, tool wear, and machined surfaces' roughness was investigated. This research was carried out for polycrystalline diamond wedges (PCD), ceramics and sintered carbide wedges with coatings and uncoated ones. The results obtained with the laser assisted machining were compared with results obtained in conventional turning.

Keywords: laser-assisted machining, polycrystalline diamond, technical ceramics, metal matrix composites, cemented carbides

1. Introduction

The metal matrix composites as well as Si_3N_4 ceramics are important materials with many engineering and medical applications. However, the high hardness (2125HV) and brittleness of ceramics and the abrasive characteristics of the reinforced particulates in metal matrix composites (MMC) make serious difficulties when machining [1–3].

Mechanical and physical properties like high thermal resistance, high hardness, good corrosive resistance and chemical stability have encouraged use of ceramics and SiC reinforced aluminium-based composites in several engineering applications. The brittle and hard nature of these ceramics makes them difficult to machine using conventional techniques and damage caused to the surface while machining affects efficiency of components. Laser-assisted machining (LAM) has recently emerged as a potential technique for attaining high material removal rates.

MMCs and silicon nitride are increasingly attractive for engineering applications because of their superior combination of properties such as high strength, hardness, good corrosive resistance, and wear resistance. These materials are finding potential applications in the manufacture of automotive components such as some elements of cars, aerospace and medical [4, 5]. However, because of the high hardness of ceramic reinforcement, conventional turning and diamond machining, which represent the most widely used machining methods, currently provide the only options for machining metal matrix composites to the required accuracy. Even for the cutting wedges made of polycrystalline diamond and cubic boron nitride the tool wear is intense [3, 6]. Nevertheless, this technique involves low material removal rates and high tool wear, which result in high machining cost. Therefore, there is still a demand for hard to machine materials processing methods capable of enhancing high material removal rates, improving tool wear, and increasing the surface quality of the workpiece [7–9].

One way to improve the machinability of difficult to cut materials is to employ the thermal softening ability of a heat source to fluxing the material. The heat source is focused in front of a cutting tool to soften the workpiece material just ahead of the cutting tool thereby lowering the forces required to cut the material [1]. The technology is called a hybrid process of the machining, where the material is heated via laser irradiation and soft surface layer is machined by defined cutting edge of the wedges. This makes the material softer and easier to plastic deformation. In comparison with conventional machining this method significantly increases wedges durability [1, 7, 10–13]. LAM reduces the tool wear and cost of machining by reducing machine hours per part [14, 15]. In a study, Chang and Kuo [10] found a reduction of 20–22% in cutting force, which is an indicator of reducing the tool wear, and an increase in the profitability of using LAM during planning of alumina ceramics.

Research presented in this chapter builds on previous work by the author to further understand the process of laser-assisted turning. The present paper describes the experimental setup and characterization of a LAM process of a Si_3N_4 ceramics, cemented carbide layer, and metal matrix composites with a particular focus on the diamond tool wear and surface roughness.

2. Experiments

In the research, the standard metal matrix composite produced by the DURALCAN company was used as the workpiece material. The composite of a chemical composition similar to the AlSi9Mg alloy (9.2% Si, 0.6% Mg, 0.1% Fe) is reinforced with SiC particles with a particle size of between 8 to 15 μm and mass fraction about 20% (**Figure 1**). The sample has 50 mm in

diameter and 10 mm length and before LAM it was painted by absorptive coat to improve absorbability of laser beam.
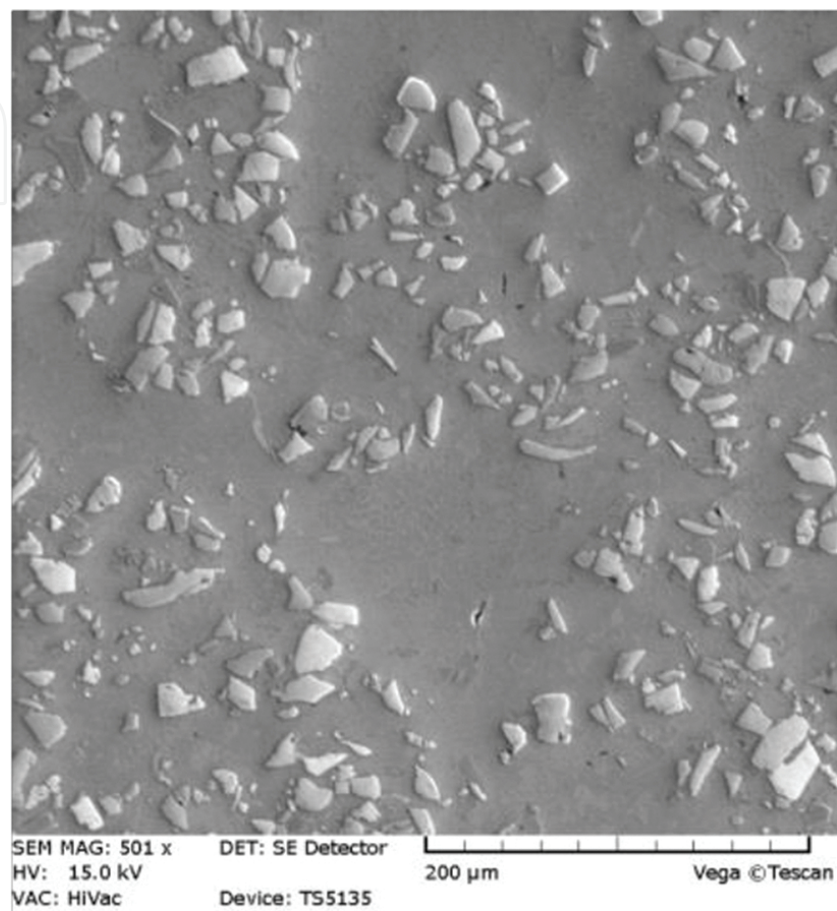

Figure 1. Microstructure of metal matrix composite used in research. The SiC particles are distributed through the matrix.

The machining tests were carried out on TUM 35D1 lathe with infinitely variable adjustment of rotational speed.

In order to determine the laser heating conditions for materials, there were materials that have been investigated, presented in **Table 1**.

Kind of masterials	Hardness	Grain size (µm)
AlSi9Mg (9.2% Si, 0.6% Mg, 0.1% Fe) +20% SiC	77 HRB	8–12
Cemented carbide (60% WC, 40% NiCr)	3000±500 HV	40–100
Si_3N_4	1809±40 $HV_{0.5}$	2–4

Table 1. Characteristics of the samples.

The example of laser-assisted turning of ceramics Si_3N_4 is illustrated in **Figure 2**.

The experimental setup applied for turning of Si_3N_4 ceramics is presented in **Figure 3**, while the setup for turning of MMC in LAM conditions is presented in **Figure 4**.
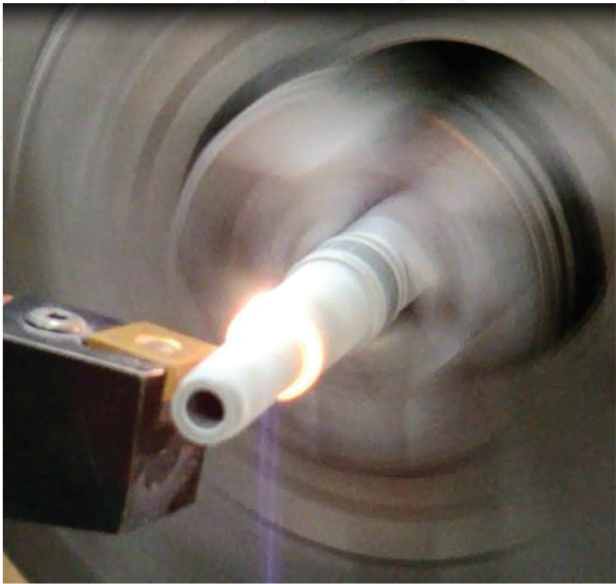

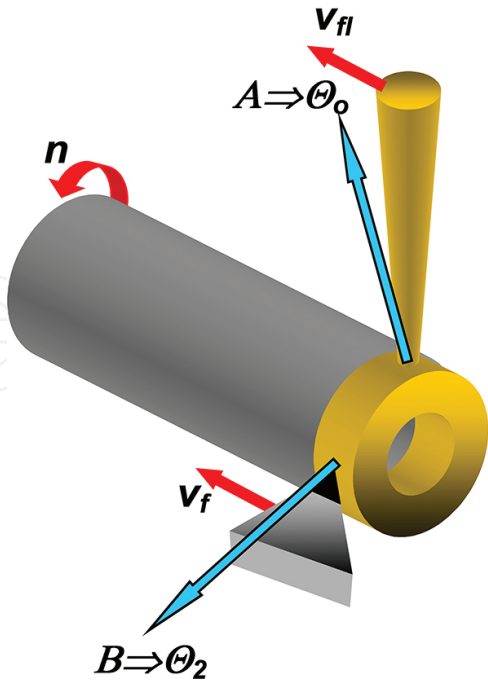**Figure 2.** View of ceramics Si_3N_4 (Ø14×4.5×104mm) heated by laser beam.

Figure 3. The scheme of experimental set-up. Ceramics turning with LAM, designations: A—heating area by laser beam, B—zone of machining, d—workpiece diameter [1].

The 30 degree angle between heated area and zone of machining was selected **Figure 4**. The tools wear were measured for each trial of experiment. The surface roughness of the sample was measured by surface analyzer (Hommel T500). The machined surface finish was characterized by the average arithmetic roughness (Ra parameter). Tool wear was measured on the primary flank face by the optical microscope.
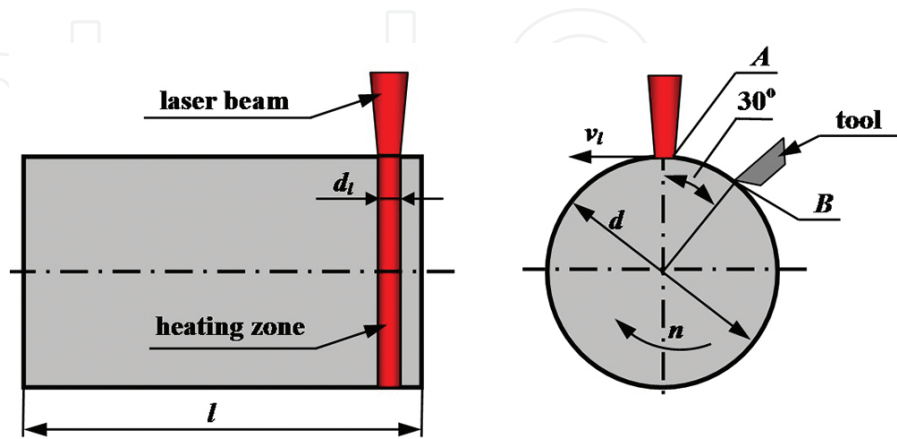

Figure 4. The scheme of experimental setup. (a) MMC laser-assisted turning, (b) Ceramics turning with LAM, designations: A—heating area by laser beam, B—zone of machining, d—workpiece diameter, d_l—laser beam diameter [1].

LAM was carried out with a 2.6 kW CO_2 laser (2.6kW Trumpf, type TLF2600t).

The workstation for Si_3N_4 ceramics was equipped with remotely controlled temperature measurement system, which works on the base of infrared detection of irradiation. The measurement data logging gives an opportunity of on-line tracking temperatures in: θ_0—machined workpiece temperature in laser beam power spot size on the heated surface; θ_2—cutting tool point on the machined surface temperature **Figure 3**). The laser-assisted turning process was done in two steps. The ceramic bush with n rotational speed was heated in t_o period time up to reach the target of suitable workpiece temperature. The next step was the initiation of feed motion, and then the laser power spot size within wedge tool was straight moved. The constant temperature during laser-assisted turning process was ensured by dedicated computer program. The obtained θ_2 temperature data logging was compared with manual typing process temperature. The on-line program has changed laser beam power in case of appeared differences between those temperatures. The system power control was worked on the base of negative feedback.

The research was carried out for these cutting parameters:

Si_3N_4: cutting speed v_c = 10 m/min, feed rate f = 0.04mm/rev, depth of cut a_p = 0.05mm;

MMC:cutting speed v_c = 10–100m/min, feed rate f = 0.04–0.1 mm/rev, depth of cut a_p = 0.1mm;

Cemented carbide: cutting speed v_c = 20 m/min, feed rate f = 0.04 mm/rev, laser power P = 600–2600W.

The characteristics of applied edges are shown in **Table 2**.

	Type of edge material	Symbol of insert material	Coating	Insert
1	Sintered carbide inserts with fine-grain substrate	KC5510	(PVD) TiAlN	SNMG120408
2	Sintered carbide	H10S	Cemented Uncoated	SNMG120408
3	Oxide ceramics ($Al_2O_3 + ZrO_2$)	AC5	Cemented Uncoated	SNGN 120708T 02020
4	Mixed ceramics ($Al_2O_3 + TiCN$)	MC2	Cemented Uncoated	SNGN 120708T 02020
5	Polycrystalline diamond PCD	KD100	Cemented Uncoated	TPGN110304F

Table 2. Characteristics of applied edges.

3. Results

3.1. Laser surface heating

In **Figure 5**, an example of two point measurements (θ_0 and θ_2) for Si_3N_4 ceramic is presented. The slow heating process of rotating Si_3N_4 ceramics up to required and accepted θ_2 temperature into control system was done in $t = 0$- to time interval only. The system control unit was increasing laser power irradiation after switching on the v_f feed motion. The laser power irradiation and cutting tool were displaced; therefore, the laser power increase was necessary to get θ_2 constant temperature of the cutting tool point on the machined surface. As a result, the θ_0 temperature increase was noticed in the first phase. The explanation of this phenomenon
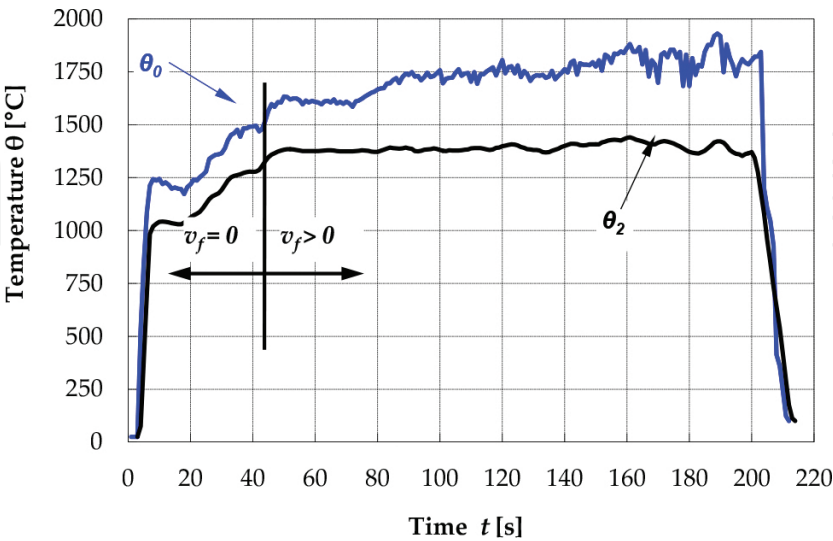

Figure 5. Temperature distributions of the θ_0 and θ_2 during laser-assisted turning within temperature control.

is low thermal conductivity of heated ceramics; therefore, the first phase heating time during feed on required higher laser power irradiation level.

In **Figures 6** and **7** the courses of MMC surface temperature during heating with turning kinematics are shown. Temperature in heated area by laser beam succumb to stabilization (**Figure 7**), varying with the increase of temperature in time on B area (**Figures 6** and **7**). This is due to the heat accumulation in the examined sample. Range of temperature Θ_1 equals about 30°C (**Figure 6**), varying based on the different thickness of absorption layer (gouache) on sample surface as well as differences of surface texture for example surface roughness. There is noticeably varied increase of temperature Θ_1 from 223 to 510°C (**Figure 7**) in plan machining area (B).
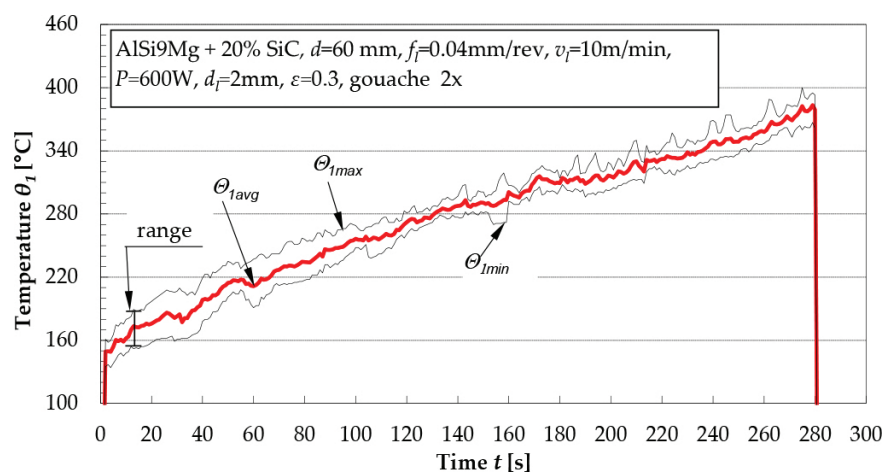
Figure 6. Courses of temperature Θ_1 (B zone) during heated MMC by laser beam with maximum and minimum values.
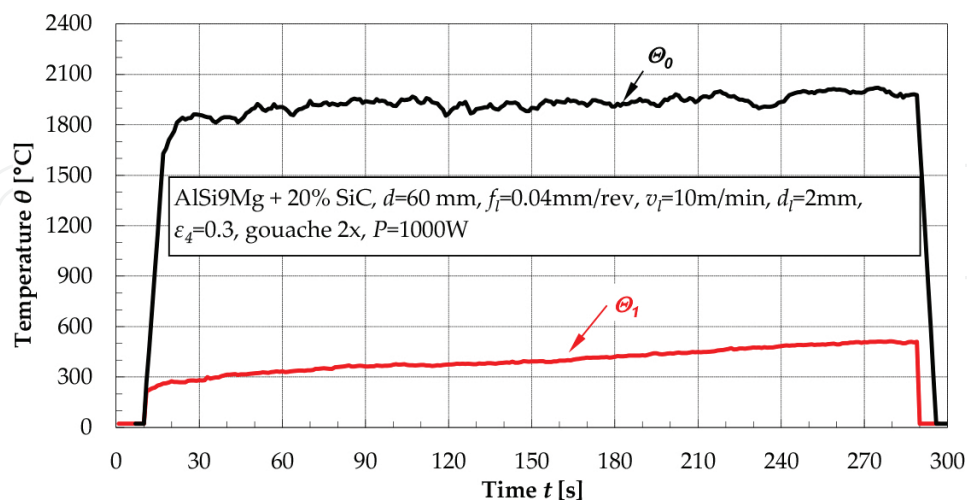

Figure 7. Exemplary courses of temperature Θ_1 in A (Θ_0) and B (Θ_1) areas during laser heating metal matrix composite.

The **Figure 8** shows the temperature course in time for cemented carbide sample, close to the place of the incidence of the laser beam for different laser powers with heating speed of

20 m/min. The courses of the temperature measurement are stable and do not increase over time.
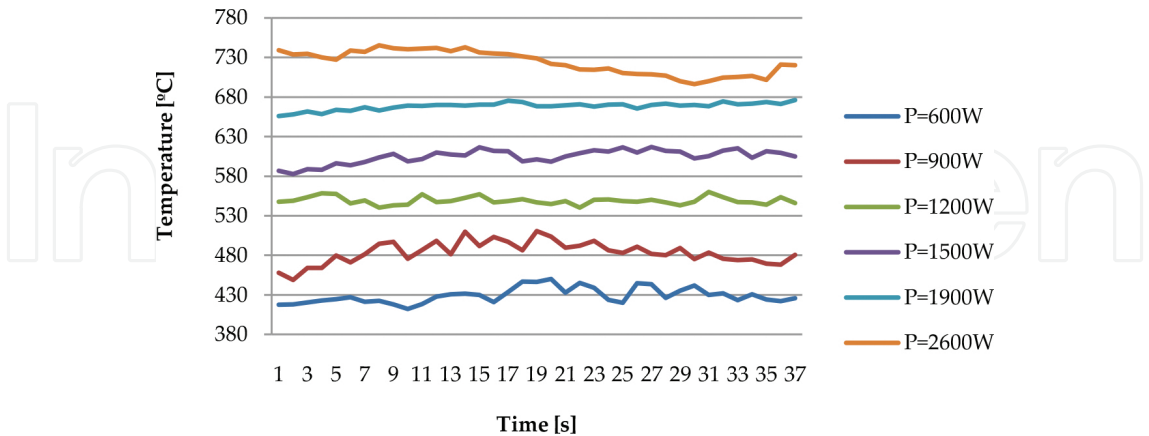

Figure 8. The temperature profile over time for cemented carbide with different laser power in place of the heating area v_f= 20 m/min.

3.2. Tool wear

In **Figure 9**, the investigation results are shown. The laser heated machined ceramic surface temperature increase has decreasing effect on the **VB$_c$** wear insert tool indicator and the lowest values of it for θ_2 = 1400–1500°C temperatures were noticed. The value of wear inserts tool in those temperatures is more than 5 times lower than wear without using laser heating of machined layer. The inserts tool abrasive and adhesive wear symptoms were observed in the range of investigated temperatures. However, thermal wear symptoms were not apparent. The θ_2 = 1400°C as an optimal temperature was selected for further investigation of machined surface laser heating, because the selection of θ_0 > 2000°C results in an evaporation risk on machined material.
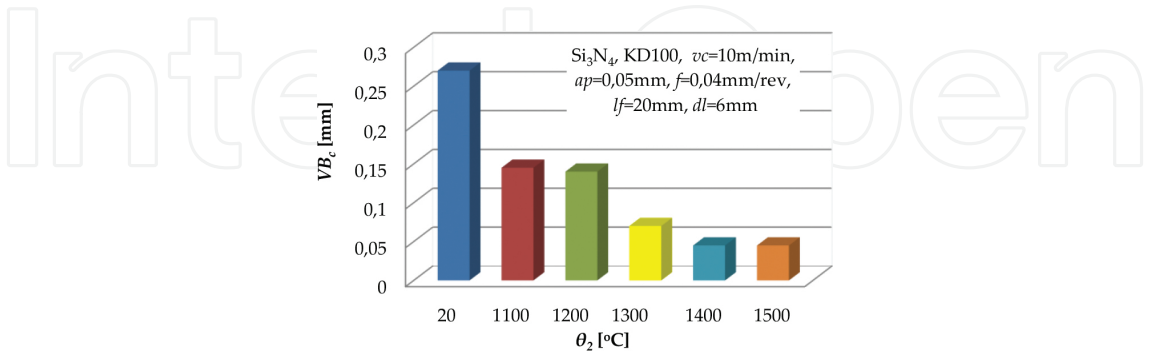

Figure 9. Polycrystalline diamond (PCD) inserts wear in function of the machined surface temperature after 1 tool pass.

In **Figure 10**, wear distributions of investigated tool wedges during laser-assisted turning of ceramic process for selected temperature are presented. The value of the tool insert wear

indicator in the range of 1300 and 1400°C temperatures is diversified for the first few passes. However after the next few passes, the difference becomes smaller and after 10 minutes time of machining is insignificant. It could be expected that in real-time analysis the presented wear plots below will look a little bit different, because high temperature exposure of the tool wedges will be much longer than investigated time interval.
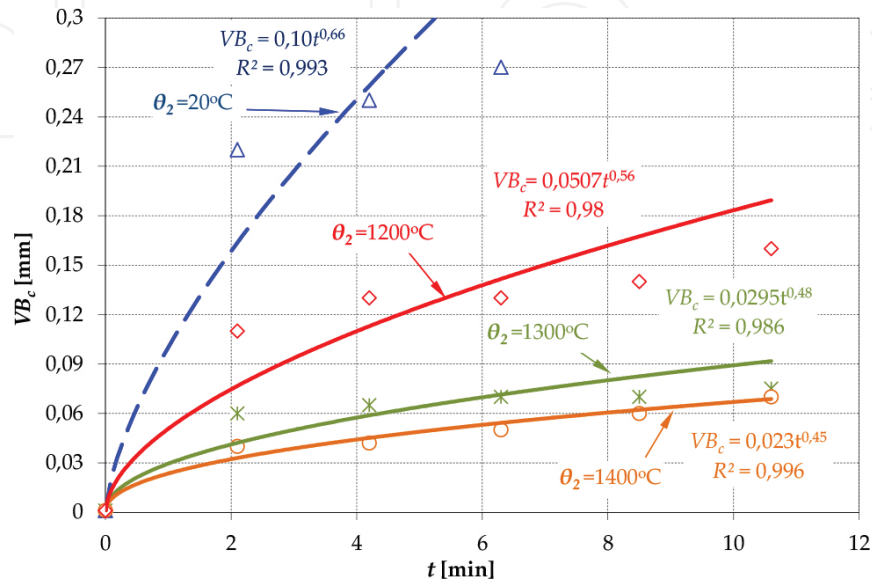

Figure 10. Polycrystalline diamond (PCD) wedges wear distributions during laser-assisted turning process for differ-ent Si_3N_4 machined surface temperature. The applied parameters: v_c = 10 m/min, a_p = 0.05 mm, f = 0.04 mm/rev.

The results of the influence of the heating temperature (θ_2=1400°C) cut layer of ceramic Si_3N_4 on tool wear for different wedges are shown in **Figure 11**. It can be observed that the lowest value of tool wear was for PCD and the largest for ceramics wedges.
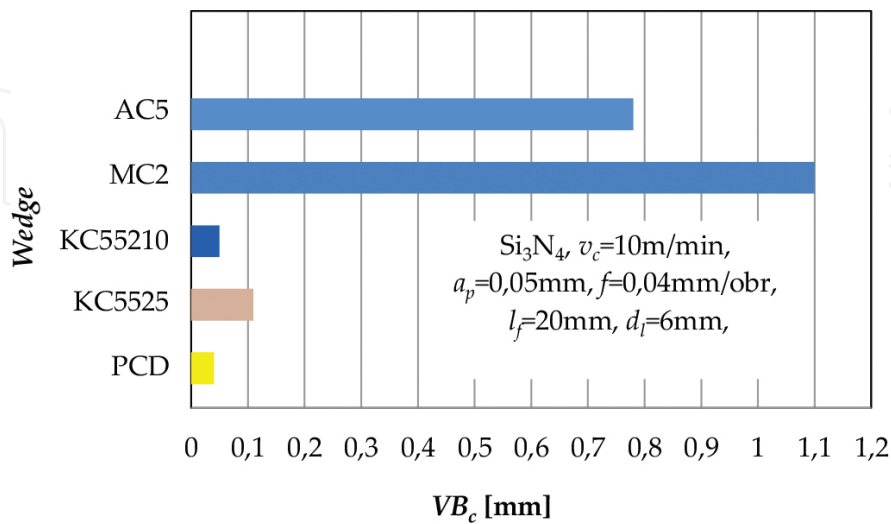

Figure 11. Tool wear for different cutting wedges.

Wedge wear of the AC5 in temperature 1300°C was minimum and at three times lower than at room temperature (**Figure 12**). Tool wear of ceramics as compared to the cemented carbide was very large and the wedges are classified as unable to withstand such difficult conditions.
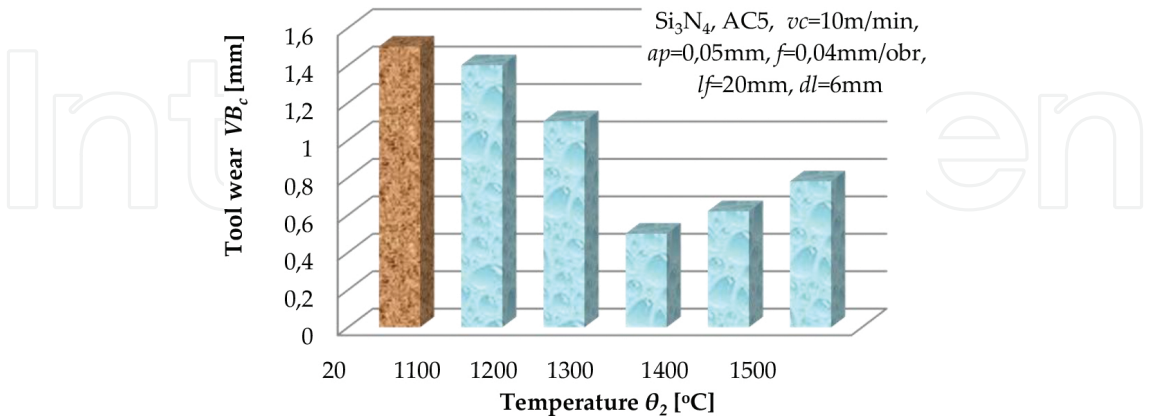

Figure 12. Ceramics AC5 wedge wear in function of machining of the machined surface temperature Θ2.

Figure 13 shows the influence of LAM on the flank wear during turning of Al-SiC metal matrix composites. These results indicated that as a consequence of heating the wedge wear was decreased significantly for tested tools. In **Figure 13**, it can be observed that for LAM, wedge wear is about 31% lower in comparison to conventional turning with cemented carbide and 35% for polycrystalline diamond wedge. However, it is equally important to note that when comparing all results, a laser power of 1000W is the most likely reason giving the optimum tool wear when machining Al/SiC metal matrix composite. The research confirmed the thesis that the softening of the matrix material composite allows pushing in or sliding hard reinforcing particles in the surface layer thus reducing the wear of cutting wedges.
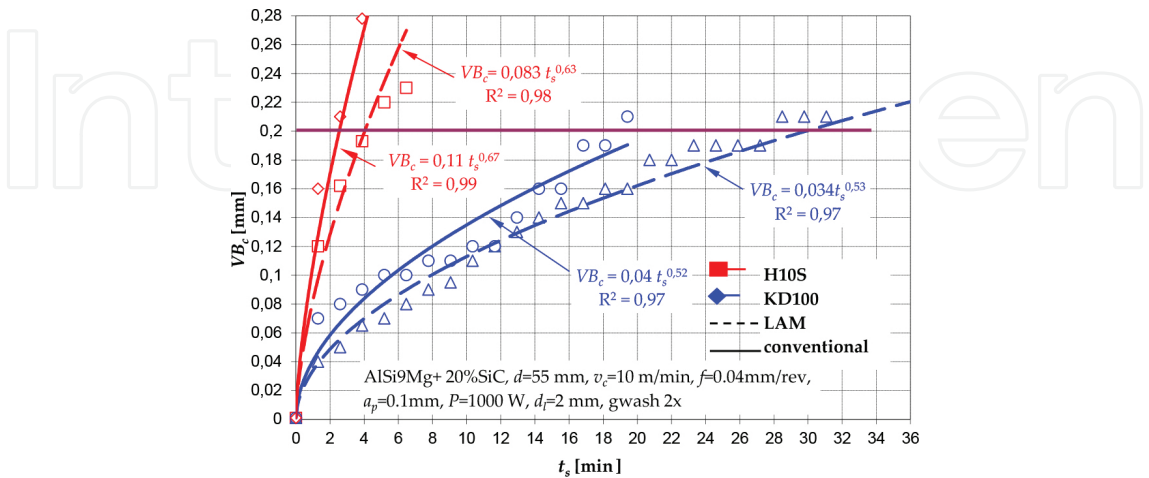

Figure 13. The evolution of the tool wear VBc indicator during turning the metal matrix composites with different feed rate values, the diamond and cemented carbide wedges.

The main wear pattern was observed as regular flank wear. Flank wear is due to the abrasive action of the reinforced particles presence in the MMC. The hard particles SiC of hardness about 2600HV grind the flank face of the cutting tools in similar way as a grinding wheel during machining of materials.

3.3. Machined surface roughness

One of the important indexes of finished product is surface quality. For these experiments, average machined surface roughness values of LAM were found to be lower than those of the conventional turning for all tested tools.

Machined surface roughness of Si_3N_4 ceramics after turning with polycrystalline diamond wedges (PCD) indicates some regularities (**Figure 14**). The increase of temperature in cutting layer (in majority of reported cases) increases the height of roughness profile. The increase of tool wear at the different cutting temperatures does not change this regularity. Therefore a thesis can be stated, that microroughness surface height is not related to the cutter's microgeometry, but temperature of cutting layer in laser-assisted process.

Similar to courses described earlier were those obtained for the turning with cemented carbide wedges KC5510 (**Figure 16**).
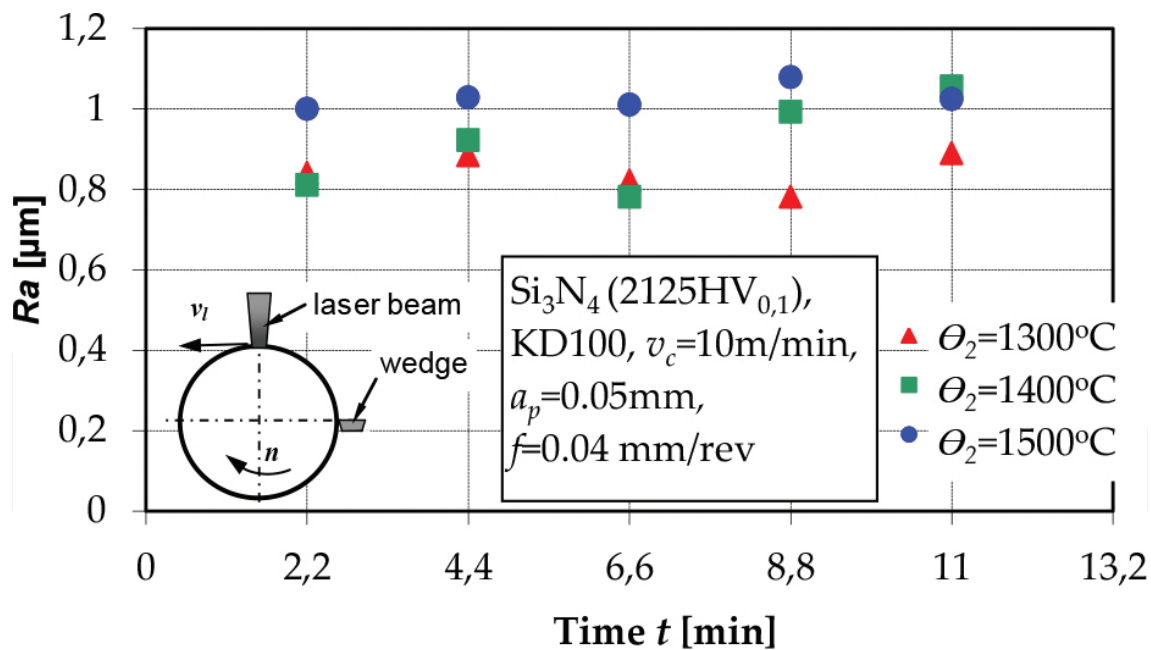

Figure 14. Machined surface roughness in function of machined Si_3N_4 surface temperature, after turning with PCD polycrystalline diamond wedges.

(for $t_s \approx 2$ min) Si_3N_4 ceramic machined surface, it can be noticed that in the analyzed temperature range of cutting layer, surface roughness after turning with carbide KC5510 cutter is higher than that generated for the PCD wedge (**Figure 15**).
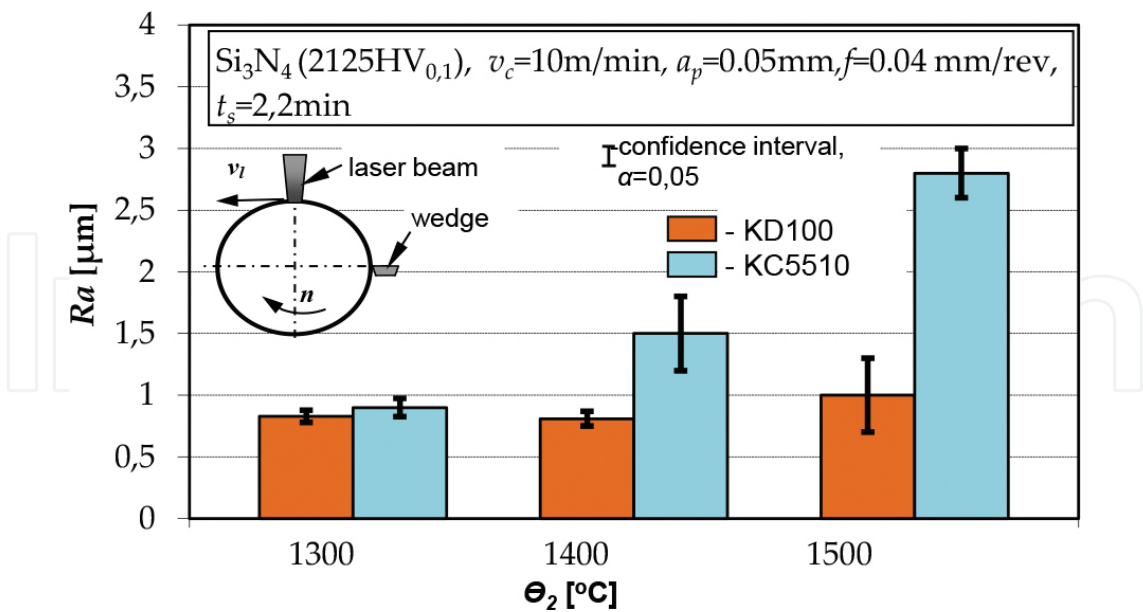
Figure 15. The initial roughness (ts ≈ 2 min) of machined surface for difference temperatures of machining layer after PCD and KC5510 wedges turning.

The increase of the machined surface roughness of Si_3N_4 ceramics, together with the temperature growth, can be explained by changes in the decohesion mechanism of the workpiece. Lower temperatures of the process are dominated by a brittle cracking, while the higher ones are dominated by a plastic flow of work material. Major role in the creation formation of machined surface during turning with a laser heating of a cutting layer have microchips with tendency to adhere to workpiece, and thus to increase in the height of microroughness.
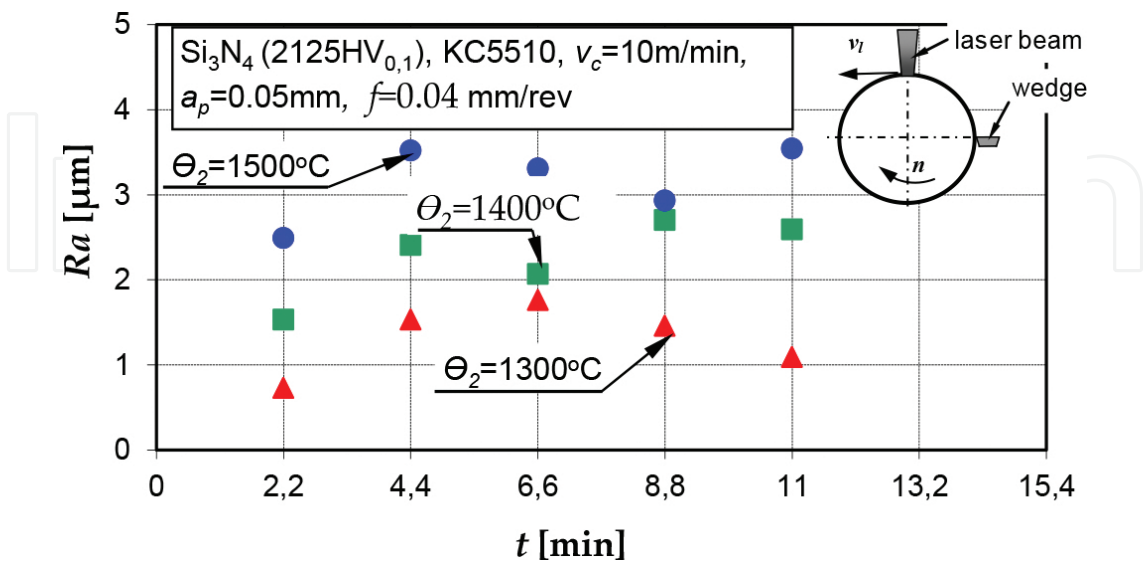

Figure 16. Machined surface roughness distributions during laser-assisted turning process for different machined surface Si_3N_4 temperature, after turning with KC5510 carbide wedges.

The higher temperature of ceramic materials in machining layer during the LAM process improves the cutting ability evaluated by a tool wear [11] but has an adverse effect on quality of machined surface.

Average width of the profile roughness grooves (*RSm*) are, in the investigated range, higher than the feed rate values (**Figure 17**). This indicates difficulties in formation mechanism of the machined surface, inducing serious disturbances in kinematic-geometric projection of the cutter into the workpiece.
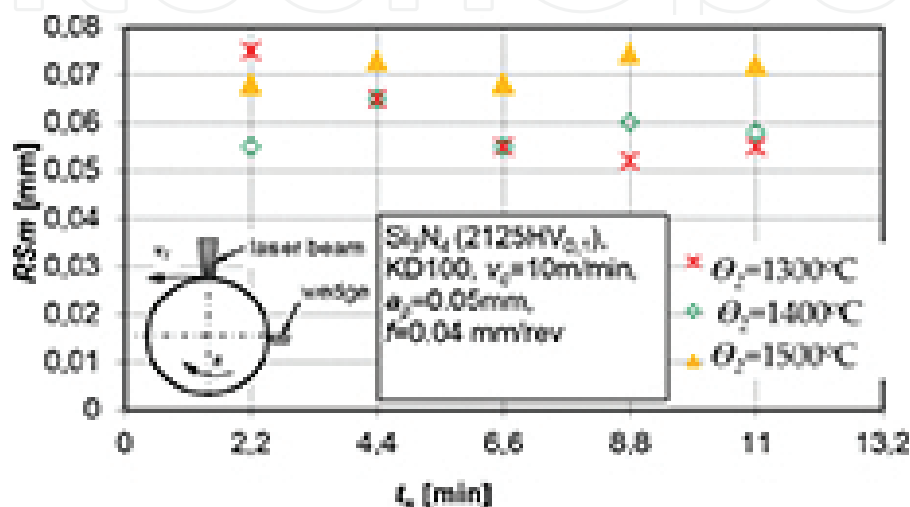

Figure 17. Machined surface roughness RS_m parameter distributions for the different machined Si_3N_4 surface temperature, after turning with PCD wedges.

Figure 18 shows that surface texture has a random character without any wedge mapping in the investigated feed range (f = 0.04 mm/rev). However, the graph of 3D profile (**Figure 18a**) and power spectral density (PSD) graph reveal that dominant peak is different from the applied feed rate (**Figure 18b**).
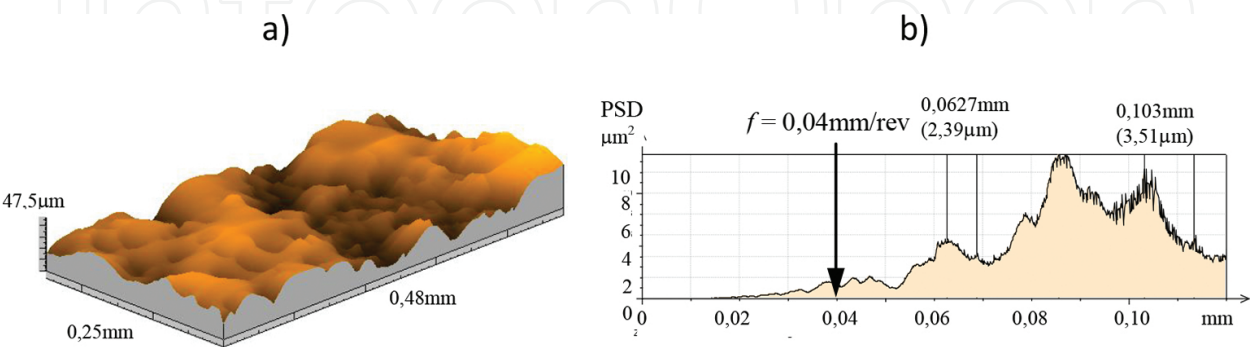

Figure 18. View of laser-assisted turning Si_3N_4 ceramics by polycrystalline diamond (PCD) wedges. (a) surface texture and (b) power spectrum density of the roughness profile. The applied parameters: θ_2 = 1400°C, v_c = 10 m/min, a_p = 0.05 mm, f = 0.04 mm/rev.

Nevertheless, in case of turning with KC5510, clear microstructure's orientation can be seen (**Figure 19**), which is attributed to the kinematic-geometric projection of the cutter into the workpiece. This observation is confirmed by a PSD diagram (**Figure 19b**), where the modal value of profile component has a frequency close to the feed rate.
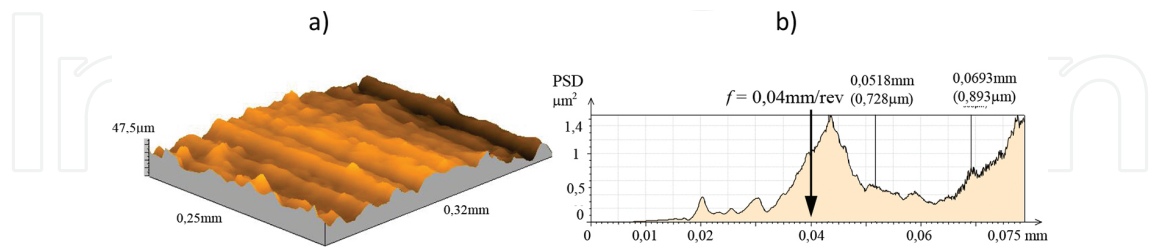

Figure 19. View of Si_3N_4 ceramics surface texture (a) and power spectrum density of the roughness profile (b) after laser-assisted turning within carbide (KC5510) wedges. Parameters: θ_2 = 1400°C, v_c = 10m/min, a_p = 0.05mm, f = 0.04mm/rev.

The machined surface roughness is one of the most important quality indicators of the MMC materials. **Figure 20** shows the influence of LAM on the machined surface roughness Ra parameter, during turning of Al/SiC metal matrix composite with different cutting wedges. Significant differences in the roughness of machined surface were observed for the laser-assisted and conventional turning (P= 0 W) with the carbide wedges. However, for the conventional turning, it is seen that average machined surface roughness value is higher than that obtained for the LAM. It could be explained by the fact that, in conventional turning, SiC particles were pushed through the soft matrix or pushed out of matrix during machining. Consequently, cracks and pits were formed on the machined surface (**Figure 10**), which are inducing poor surface finish. During hybrid machining, laser heated layer is being cut in the liquid or semi-liquid state, so that fills the grooves in the machined surface generated after plowing or crumbling out the reinforcement particles. This mechanism reduces the average height of machined surface roughness.
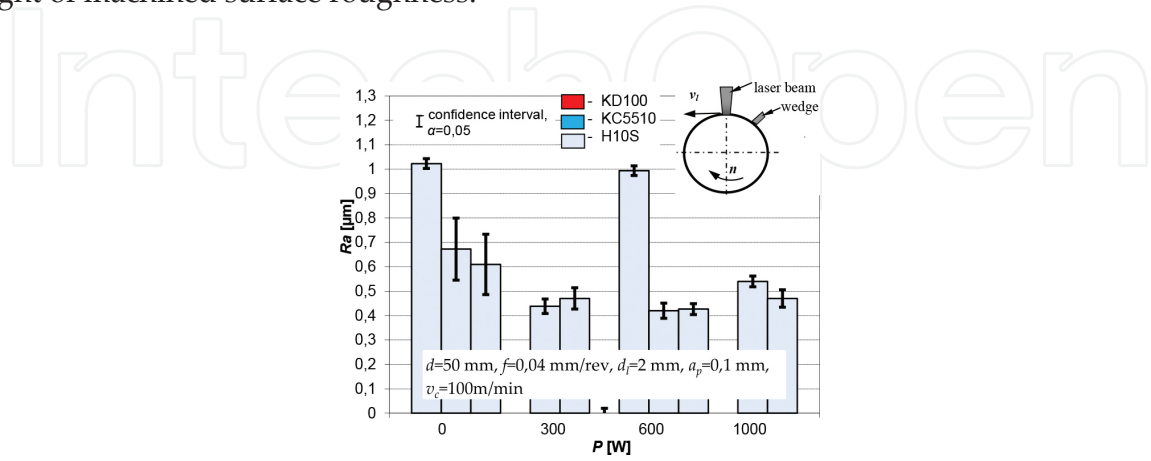

Figure 20. The influence of a laser's beam power on machined surface roughness Ra after LAM and conventional turning of aluminum-ceramic via different cutting wedges material.

The analysis of power spectrum density (PSD) of the roughness profile revealed that machined surface texture has random character with the significant disturbances of the cutting edge kinematic-geometric projection. The PSD chart has dominant component different from the applied feed rate. The analysis of power spectrum density for different values of feeds (f_1 = 0.07 mm/rev, f_2 = 0.1 mm/rev) reveals significant disturbances of the cutting edge kinematic-geometric projection (**Figure 21**).

In **Figure 21b**, the orientation of surface texture was observed as a result of turning kinematics; however, a power spectrum density diagram did not reveal a component related to the employed feed rate. **Figure 21a** and **21b** shows a cavity created after crumbling out the SiC particles from metal matrix.
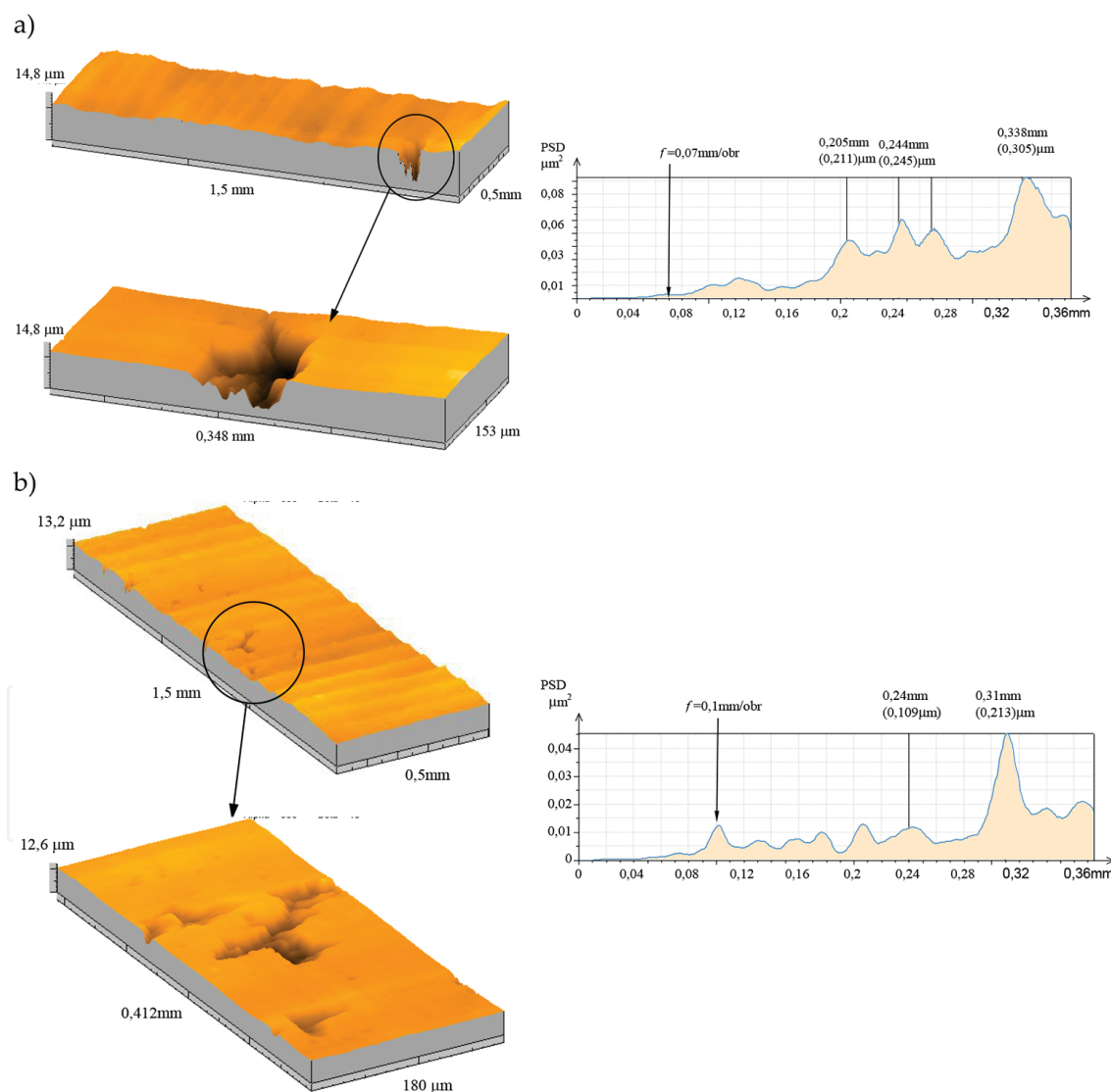

Figure 21. 3D topographic images (machined surface of metal matrix composite and power spectrum density) of surface roughness profiles after conventional turning of non-coated carbide H10S wedge for feed rate: (a) f = 0.07 mm/rev, (b) f = 0.1 mm/rev.

However, in the case of conventional turning, there was an increase in average surface roughness for analyzed sample in comparison with LAM. The formation of grooves on the sample as a result of moving of SiC particles by cutting tool is a major cause of the deterioration of surface roughness with traditional turning. With a LAM the temperature in cutting zone increased and leads to weakening the connections between the SiC particles and aluminium matrix. In most cases, it causes pushing the particle outside or in to the aluminium alloy. The same observation had Altinkok [16] in research.

Figure 22 shows a comparison of the surface profiles of the machined surface by conventional cutting and LAM. The profiles show the difference of surface finish achieved.
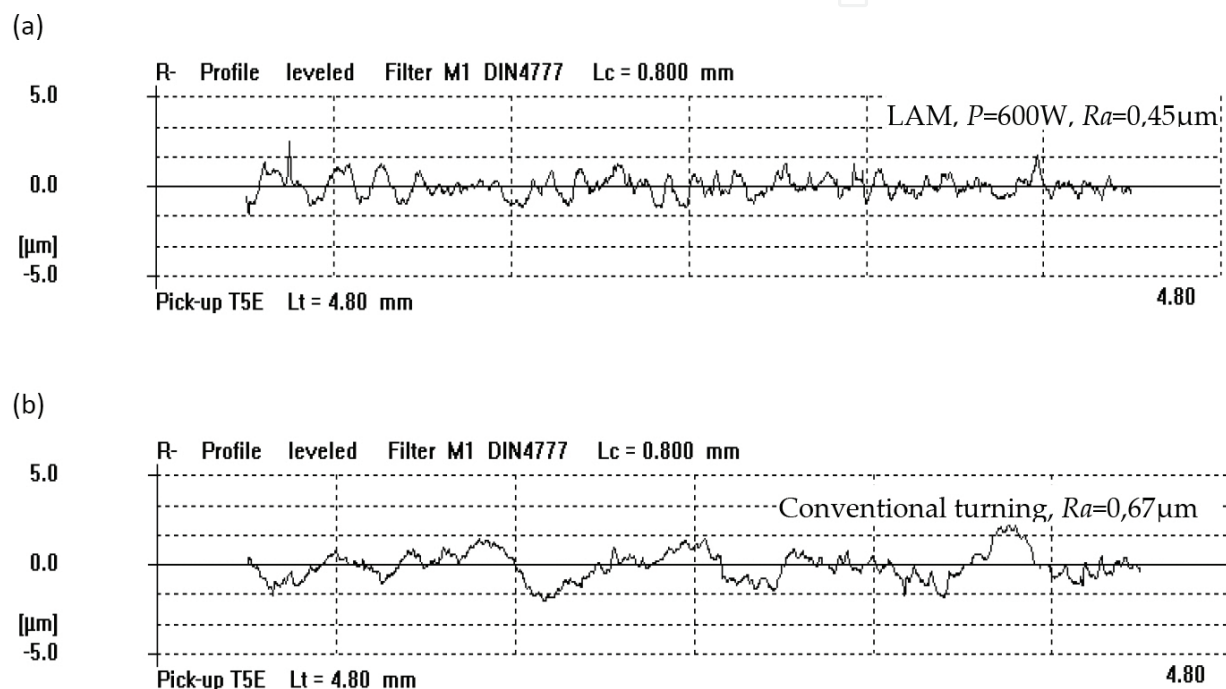
(a)

R- Profile leveled Filter M1 DIN4777 Lc = 0.800 mm

LAM, P=600W, Ra=0,45μm

Pick-up T5E Lt = 4.80 mm

(b)

R- Profile leveled Filter M1 DIN4777 Lc = 0.800 mm

Conventional turning, Ra=0,67μm

Pick-up T5E Lt = 4.80 mm

Figure 22. Comparison of machined surface roughness profiles for the same cutting conditions. Laser Assisted Machining (a) and conventional turning (b)

4. Conclusions

Laser enhanced conventional turning to heat the cutting materials, as well as to change the microstructure or locally harden the material in front of the cutting tool. This process is carried out in order to facilitate the machining due to its softening and change of the workpiece's deformation behavior. The local temperature of the material in the shear deformation zone plays an important role in the thermally enhanced machining process.

The investigations on laser-assisted turning of difficult to cut materials confirmed that laser heating of the machined surface causes significant improvement in turning process, which is estimated by tool wear and surface roughness indicators.

The low tool wear intensity in a suitable temperature is crucial for increasing the tool life. This opportunity enables the significant reduction of cost tool production.

The flank face wear was observed during laser-assisted and conventional turning. The abrasive tool wear mechanism is dominant in turning of these materials. Turning with laser heating improves machined surface roughness in comparison with conventional turning for all examined wedges.

Acknowledgements

Author details

Damian Przestacki

Address all correspondence to: damian.przestacki@put.poznan.pl

Poznan University of Technology, Poznan, Poland

References

[1] Przestacki D., Jankowiak M. Surface roughness analysis after laser assisted machining of hard to cut materials. Journal of Physics: Conference Series. 2014; 483: 012019, Published online: 28 March 2014.

[2] Przestacki D. Conventional and laser assisted machining of composite A359/20SiCp. Procedia CIRP. 2014; 14: 229–233.

[3] Davim J. P., Baptista A. M. Relationship between cutting force and PCD cutting tool wear in machining silicon carbide reinforced aluminium, Journal of Materials Processing Technology. 2000; 103: 417–423.

[4] Naher S., Brabazon D., Looney L. Computational and experimental analysis of particulate distribution during Al–SiC MMC fabrication. Composites: Part A. 38; 2007; 38: 719–729

[5] Bassani P., Capello E., Colombo D., Previtali B., Vedani M. Effect of process parameters on bead properties of A359/SiC MMCs welded by laser. Composites: Part A. 2007; 38: 1089–1098.

[6] Davim J. P. Diamond tool performance in machining metal-matrix composites. Journal of Materials Processing Technology. 2002; 128: 100–105.

[7] Skvarenina S., Shin Y. C. Laser-assisted machining of compacted graphite iron. Journal of Machine Tools and Manufacture. 2006; 46: 7–17.

[8] Manna A., Bhattacharyya B. A study on different tooling systems during machining of Al/SiC-MMC. Journal of Materials Processing Technology. 2002; 123: 476–482.

[9] Pramanik A., Zhang L. C., Arsecularatne J. A. Machining of metal matrix composites: effect of ceramic particles on residual stress, surface roughness and chip formation. International Journal of Machine Tools and Manufacture. 2008; 48: 1613–1625.

[10] Chang C. W., Kuo C. P. Evaluation of surface roughness in laser-assisted machining of aluminum oxide ceramics with Taguchi method. Machine Tools and Manufacture. 2007; 47: 141–147.

[11] Jankowiak M., Bartkowiak K. Machinability of laser heated silicon nitride ceramics during turning process. Proceedings of the 25th International Congress on Applications of Lasers & Electro-Optics ICALEO, Scottsdale, AZ, USA. 2006; 311–316.

[12] Ding H., Shin Y. C. Laser-assisted machining of hardened steel parts with surface integrity analysis. International Journal of Machine Tools & Manufacture. 2010; 50: 106–114.

[13] Ding H., Shen N., Shin Y. C. Thermal and mechanical modeling analysis of laser-assisted micro-milling of difficult-to-machine alloys. Journal of Materials Processing Technology. 2012; 212: 601–613.

[14] Sun S., Brandt M., Dargusch M. S. Thermally enhanced machining of hard-to-machine materials-a review. International Journal of Machine Tools & Manufacture. 2010; 50: 663–680.

[15] Dandekar C. R., Shin Y. C. Multi-scale modeling to predict sub-surface damage applied to laser-assisted machining of a particulate reinforced metal matrix composite. Journal of Materials Processing Technology. 2013; 213: 153–160.

[16] Altinkok N. Investigation of mechanical and machinability properties of Al2O3/SiCp reinforced Al-based composite fabricated by stir cast technique. Journal of Porous Materials. 2015; 22 (6) DOI: 10.1007/s10934-015-0048-0.